Seventh International Conference on CFD in the Minerals and Process Industries
CSIRO, Melbourne, Australia
9-11 December 2009

SCREW CONVEYOR PERFORMANCE: COMPARISON OF DISCRETE ELEMENT MODELLING WITH LABORATORY EXPERIMENTS

Philip J. OWEN and Paul W. CLEARY

CSIRO Mathematics, Informatics and Statistics, Clayton, Victoria 3168, AUSTRALIA

ABSTRACT

Screw conveyors are used extensively in agriculture and processing industries for elevating and/or transporting bulk materials over short to medium distances. They are very effective for conveying dry particulate solids, giving good control over the throughput. Despite their apparent simplicity, the transportation action is very complex and designers have tended to rely heavily on empirical performance data. In our previous work, we explored how screw conveyor performance is affected by its operating conditions (such as: the rotational speed of the screw, the inclination of the screw conveyor, and its volumetric fill level). In that work, the predicted mass flow rate was in excellent agreement with experimentally measured values for the horizontal and vertical configurations across the full range of screw rotation rates. Although the throughput predictions for the screw conveyor inclined at 30° and 60° followed the same qualitative trend, there were moderate differences between the DEM and experimental results. In this paper, we use the Discrete Element Method (DEM) to examine how variations of particle properties (such as: particle shape, particle-particle and particle-wall friction) influence the performance of the screw conveyor. The primary focus of our study is comparing predicted mass flow rates with experimentally measured values. The secondary focus is to study how other performance measures (such as: particle speeds and power consumption) vary due to changes in the properties of the particles.

INTRODUCTION

Screw conveyors are widely used for transporting and/or elevating particulates at controlled and steady rates. They are used in many bulk materials applications in industries ranging from industrial minerals, agriculture (grains), pharmaceuticals, chemicals, pigments, plastics, cement, sand, salt and food processing. They are also used for metering (measuring the flow rate) from storage bins and adding small controlled amounts of trace materials (dosing) such as pigments to granular materials or powders. If not designed properly for the transported material, problems experienced include: surging and unsteady flow rates, inaccurate metering and dosing, inhomogeneity of the product, product degradation, excessive power draw, high start-up torques, high equipment wear and variable residence time and segregation.

A summary of current design methods and problems experienced for screw conveyors can be found in Bortolamasi and Fottner (2001). The description of the theoretical behaviour of screw conveyors can be found in articles by Yu and Arnold (1997), and Roberts (1999). DEM modelling of particulate flow in a screw conveyor was first reported by Shimizu and Cundall (2001). They examined the performance of horizontal and vertical screw conveyors and compared their results with previous work and empirical equations. Owen et al. (2003) introduced the use of a periodic slice model to explore the performance of a long screw conveyor. Cleary (2004) used DEM to study draw down patterns from a hopper by a 45° inclined screw conveyor. This work was extended by Cleary (2007) to examine the effect of particle shape on the draw down flow from the hopper and on the transport characteristics of the screw conveyor.

In our previous work, Owen and Cleary (2009), the predicted mass flow rates for vertically and horizontally inclined screw conveyors were in excellent agreement with experimentally measured values. Although the throughput predictions for the screw conveyor inclined at 30° and 60° followed the correct qualitative trend, the DEM and experimental mass flow rates differ by 16% and 24% respectively for these two inclinations. In this paper we will use the Discrete Element Method (DEM) to explore these differences by looking at variations of: particle shape, particle–particle and particle–wall friction. We will also study how other performance measures (such as: particle speeds and power consumption) vary due to changes in the properties of the particles.

MODEL DESCRIPTION

DEM simulation involves following the motion of every particle and modelling each collision: inter-particle and between the particles and their environment (e.g. the internal surface of the screw casing and the surface of the rotating screw). The boundary geometry is built using a CAD package and imported as a triangular surface mesh into the DEM package. This provides unlimited flexibility in specifying the three dimensional geometries with which the particles interact. Here the particles are modelled as spheres and super-quadrics. The DEM code used here is described in more detail in Cleary (1998a&b, 2004).

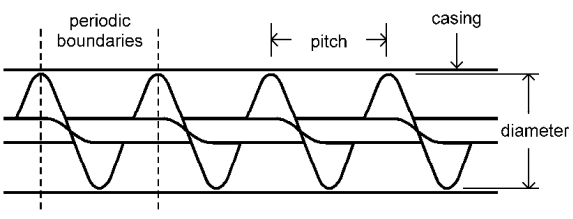

Figure 1: Standard pitch, single flight screw conveyor.

The screw conveyor used in this study was a standard pitch, single flight screw conveyor with dimensions similar to the one used by Roberts and Willis (1962) in their experiments. The pitch of the screw is defined as the

length, along the drive shaft, of one turn of the helical blade, as shown in Figure 1. A standard pitch screw has its pitch equal to the outer diameter of the helical blade.

The DEM model was simplified by applying periodic boundary conditions to a single pitch of the screw as shown in Figure 1. The diameter and the pitch of the screw were 38 mm, the diameter of the screw shaft was 13 mm, and the blade thickness was approximately 1 mm. The blade thickness for the screw in the experiments was about 3 mm (the screw was machined from a solid bar of brass). The internal diameter for tubular case was 40 mm, giving a gap of about 1mm between the outer edge of screw blade and the internal surface of the casing.

Roberts and Willis (1962) used Japanese millet seed (a grain that is very close to spherical in shape) for the dry particulates in their experiments. The size of the spherical and non-spherical (super-quadrics) particles used here ranged from 2 mm to 3.6 mm. Their sizes were uniformly distributed on a mass weighted basis, and all had a density of 700 kg/m^3 to best match the millet seed used in the experiments. The particle–particle and particle–boundary frictions used for the DEM (base case) simulations were 0.7 and 0.5, respectively, and the particle–particle and particle–boundary coefficients of restitution were 0.1 and 0.3, respectively; these are the same values used in the previous study. The maximum overlap between particles is determined by the normal spring stiffness. Typically, average overlaps of 0.1–0.5% are desirable, requiring a spring constant of 1000 N/m for this type of simulation.

A series of DEM simulations was carried out for various particle shapes, and for a range of inter-particle and particle-boundary frictions. All simulations used the same screw conveyor operating conditions, namely: a screw rotational speed of 1000 rpm, a 30% volumetric fill level, and the inclination of the screw conveyor was varied from 0° to 90° in steps of 30°.

Traditionally DEM particles are modelled as spheres in three dimensions. Here we also use super-quadrics, with general form:

$$x^N + \left(\frac{y}{B}\right)^N + \left(\frac{z}{C}\right)^N = s^N \qquad (1)$$

to describe the non-spherical particles. The power N is the shape factor, which determines the blockiness of the particle (with the shape smoothly changing from a sphere to a cube as N increases). B and C are the aspect ratios of the particle's first and second minor axes to the major axis. The particle size used in the previous study, Owen and Cleary (2009), was based on the typical size of millet, namely, 2-3 mm diameter spherical particles. Some of these DEM simulations were repeated here in the "SpA" cases (see Table 1). In this study we reduced the top size of the particles to 2.5 mm to match the Japanese millet seed used in the experiments. For cases where super-quadrics particles were used, the size of the particles was measured in two ways. In the SQA runs the particles were created so that their size in their first minor axis direction was within the specified size range. This resulted in slightly longer particles than the spheres used in the SpB runs. Fewer particles were used in order to maintain the 30% fill level. In the remaining super-quadrics runs, the particles were constructed so that their size in major axis direction was within the specified size range. As a consequence, these particles were smaller in volume and more particles were needed to obtain the 30% fill level.

DEM Particle Shape Cases	Size (mm)	Shape factor	Aspect Ratio
SpA: Spherical particles, same as previous study.	2 – 3	2	1
SpB: SpA with particles having a smaller top size.	2 – 2.5	2	1
SQA: Super-quadrics with size measured along the first minor axis	2 – 2.5	2.1 – 2.2	0.7 – 0.86
SQB: SQA with the size measured along the major axis (Base Case)	2 – 2.5	2.1 – 2.2	0.7 – 0.86
SQC: SQB with particles that are more elongated	2 – 2.5	2.1 – 2.2	0.55 – 0.7
SQD: SQC with particles that are more blocky	2 – 2.5	3.5 – 4.0	0.55 – 0.7

Table 1: Particle properties - shape parameters.

Table 1 and Table 2 summarise the range of particle shape and the range of friction values used in this study. The DEM modelling gave predictions for the changes in the screw conveyor performance due to changes in properties of the particle in terms of variations of: mass flow rate, particle speed, and power consumption.

DEM Friction Cases	Particle-Particle Friction	Particle-Boundary Friction
SQB: Super-quadrics particles (Base Case)	0.70	0.50
PPm20: Particle-particle friction reduced by 20%	0.54	0.50
PPm10: Particle-particle friction decreased by 10%	0.63	0.50
PPp10: Particle-particle friction increased by 10%	0.77	0.50
PPp20: Particle-particle friction increased by 20%	0.84	0.50
PWm20: Particle-boundary friction reduced by 20%	0.70	0.40
PWm10: Particle-boundary friction reduced by 10%	0.70	0.45
PWp10: Particle-boundary friction increased by 10%	0.70	0.55
PWp20: Particle-boundary friction increased by 20%	0.70	0.60

Table 2: Modelling conditions – Friction cases.

PARTICLE FLOW PATTERNS

Figure 2 shows particle flow patterns inside the screw conveyor for three different particle shapes after the simulations had reached steady state operating conditions.

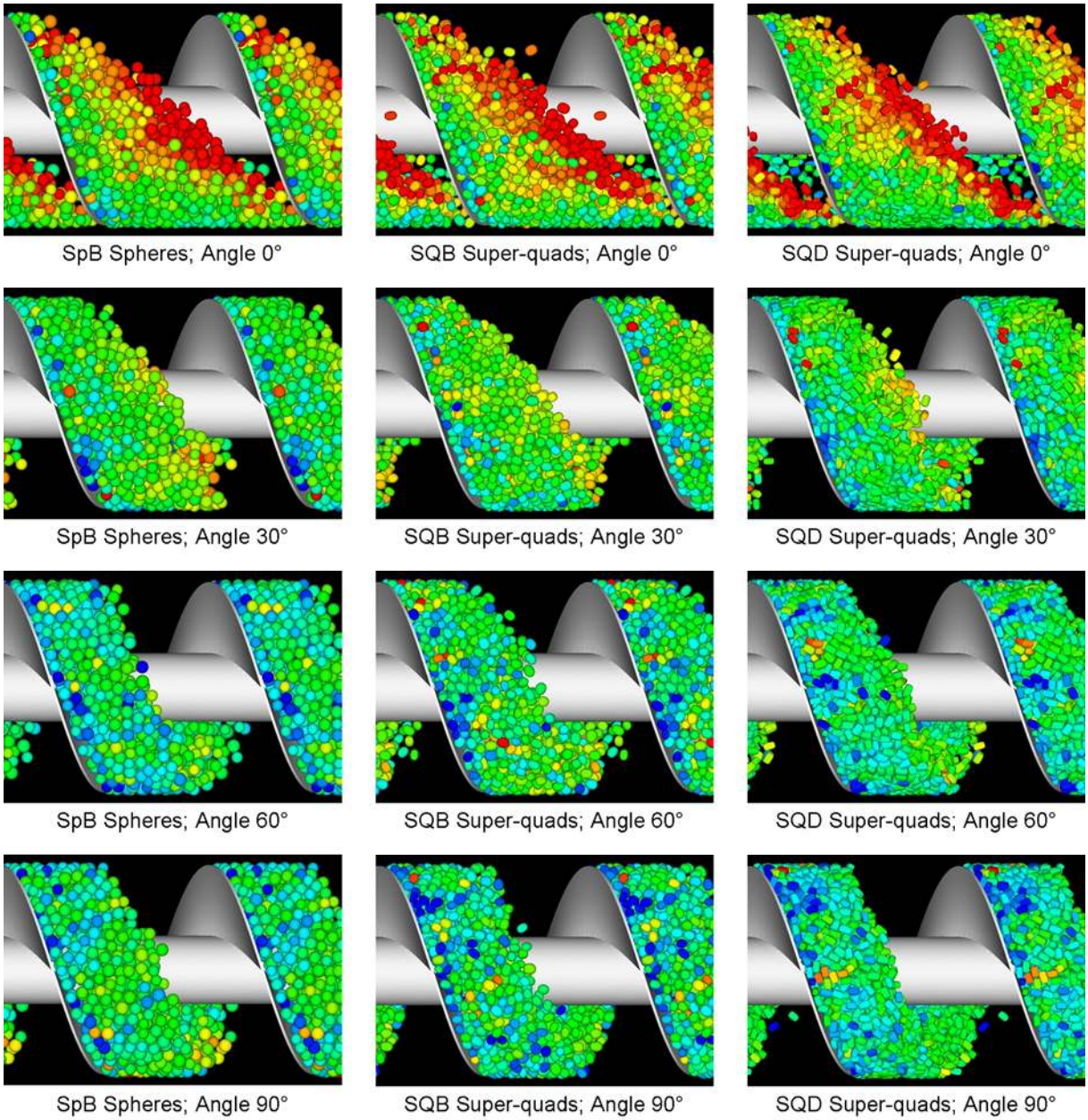

Figure 2: Particle flow patterns within the screw conveyor inclined at various angles for different particle shapes. The particles are coloured by their speed: from blue to red for 0.4 to 0.9 m/s respectively.

These steady state conditions were reached within 2–3 turns of the screw, when the power draw became quite stable. The screw conveyor operating conditions are the same for all 3 cases, namely:

- 30% by volume fill level, and
- the screw is rotating at 1000 rpm.

The left hand column of Figure 2 shows particle flow patterns for the spherical particles of case SpB; the middle column shows particle flow patterns for the super-quadratic particles of case SQB (base case); and the right hand column shows the particle flow patterns for the elongated and more "blocky" particles of case SQD. In each column there are particle flow patterns for each of the four screw conveyor inclinations modelled. Note that the angle change is implemented by changing the orientation of the gravity vector so the screw remains in the same orientation in the pictures allowing easier comparison of the changes. In Figure 2 the particles are coloured according to their speed with the slower particles ($\leq$ 0.4 m/s) being dark blue and with the faster particles ($\geq$ 0.9 m/s) coloured red.

The first row of images in Figure 2, show the particle flow patterns inside a horizontal screw conveyor. The particles form a noticeable heap against the leading face of the screw. After reaching the top of the screw most of the particles tumble down the top of the heap and a few particles fall behind the screw shaft as pictured. The particles tumbling down the free surface on the heap clearly gather speed as they go. This row of images also shows that a few particles have fallen over the shaft. This is most noticeable for the case using the blocky super-quadric particles. As the non-sphericity increases (going from left to right in Figure 2), there is little identifiable change in the particle flow patterns.

The next row of frames of Figure 2 show the changes in the particle flow patterns when the inclination of the screw conveyor is increased to 30°. The heap in front of the leading face of the screw blade has redistributed, with less material at the bottom near the casing and more material at the top. The free surface of the particles has become more aligned to the angle of the screw blade and more particles contact the leading surface of the screw. Again we see that as the non-sphericity increases there is little identifiable change in the particle flow patterns.

For higher angles, as shown in the last two rows of images, the layer of particles above the screw surface becomes more evenly spread out to produce a bed of uniform depth on top of the conveying screw. For the full range of inclinations, increasing non-sphericity of the particles has negligible effect on the particle flow patterns.

COMPARISON WITH EXPERIMENTAL RESULTS

Tracking each particle in a DEM simulation enables collection of information to measure the performance of a screw conveyor, for example: average mass flow rates, average speed of the particles, and the power draw. In our previous work, Owen and Cleary (2009), we created a DEM model of the experimental screw conveyor and compared our predicted mass flow rates with the experimental measurements of Roberts and Willis (1962). The flow rates were plotted against rotational speed for various inclinations of the screw conveyor, and are reproduced here in Figure 3. This plot also shows the theoretical maximum mass throughput of the screw conveyor, which is a linear function of the rotational speed of the screw.

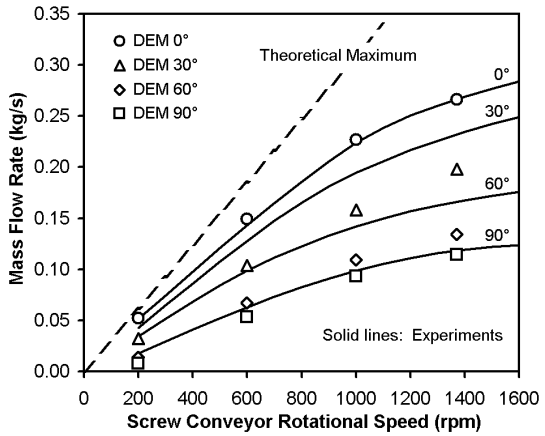

Figure 3: DEM and experiment mass flow rates from previous study by Owen and Cleary (2009).

Figure 3 shows excellent agreement between the DEM predictions and the experimentally measured mass flow rates for the horizontal (0°) and the vertical (90°) screw conveyor cases across the full range of screw rotation speeds. The DEM predictions for the screw conveyor inclined at 30° and 60° follow the same qualitative trend but there is a modest difference with the DEM mass flow rates being 16% and 24% lower, respectively. In the following sections of this paper, we will explore whether these differences are related to particle shape effects and/or particle–particle and particle–boundary frictions.

MASS FLOW RATES

The mass flow rate was determined by recording the mass of each particle that has passed through a plane perpendicular to the axis of the screw over a set time period. This plane was located half-way between the two periodic boundaries. The solid line in Figure 4 shows the average mass flow rate for the DEM Base Case versus the inclination of a screw conveyor. The DEM mass flow rate decreases strongly but linearly with increasing screw conveyor inclination until about 60°. For steeper angles, where the blade of the screw is covered by a uniform depth bed of particles, the average mass flow rate approaches a constant value.

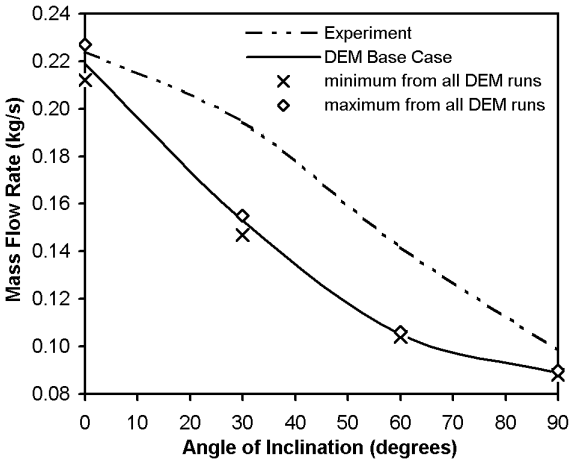

Figure 4: Mass flow rate versus conveyor inclination.

The dashed line in Figure 4 shows the mass flow rate measured in the experiments. This curve decays slowly for inclinations below 30°. Then, for steeper angles it decays strongly and linearly as the screw conveyor inclination increases to 90°. The cross and diamond symbols drawn on Figure 4 show the minimum and maximum flow rates, respectively, arising from all DEM simulation conditions in the current study. The range between the minimum and the maximum predictions for the horizontal conveyor is about 7% of the base case value. This decreases with increasing screw conveyor inclination. At the higher inclinations of 60° and 90° the range has declined to about 2%. This demonstrates that the mass flow is virtually invariant to changes in particle shape, and to changes to particle–particle and particle–boundary frictions.

TRANSPORT VELOCITIES

Figure 5 shows the average particle velocities versus conveyor inclination. Figure 5(a) shows the full range of particle shapes. Figure 5(b) shows the full range of particle-particle frictions, and Figure 5(c) shows the full range of particle-boundary friction. Each graph contains three solid curves for the DEM Base Case. The line labels speed, swirl and axial respectively refer to: the average particle speed, the average tangential or swirling component of the particle speed, and the average axial component of the particle speed. The shape of these curves for a wide range of operating conditions is discussed in detail in Owen and Cleary (2009). The main finding of that work was that as the inclination of the screw conveyor increases from the horizontal position to the vertical position:

- The average swirling speed of the particles increases.

- The average axial velocity of the particles decreases.
- These two trends broadly cancel each other to give an overall average particle speed which is fairly insensitive to inclination.

The insensitivity of the average speed masks strong structural changes in the motion between the axial and swirling velocity components driven by the change in flow pattern from a recirculating avalanching heap to a rotating bed of constant depth flowing along the screw.

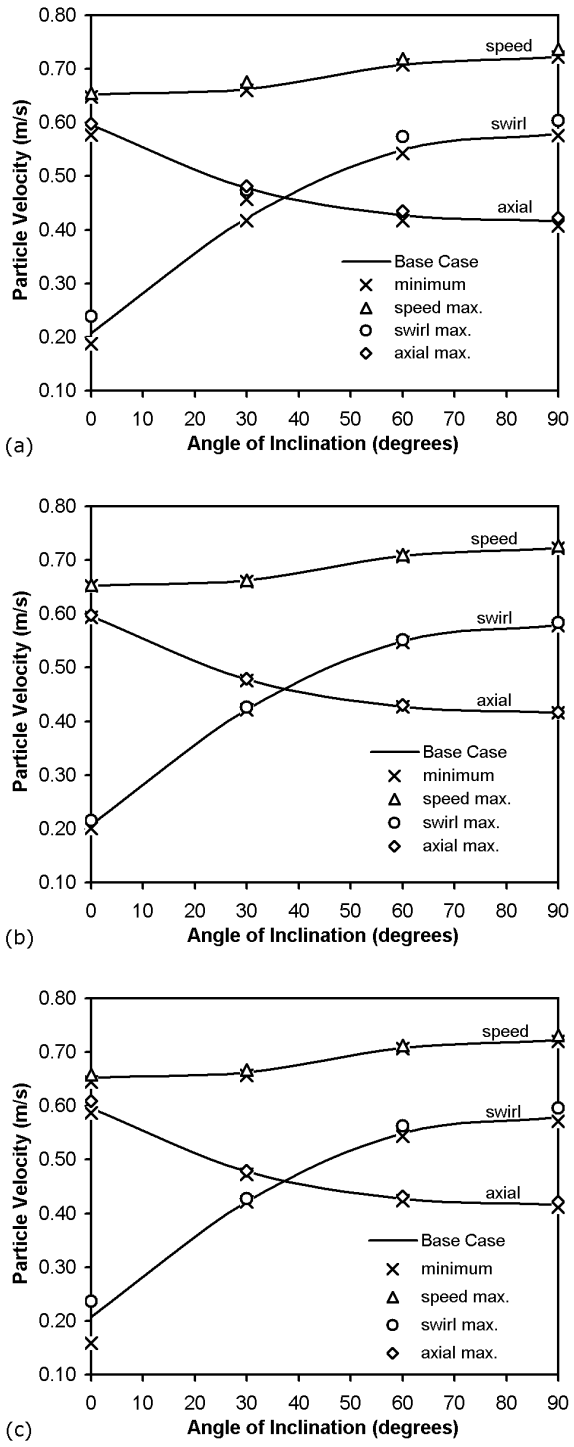

Figure 5: Particle velocities versus conveyor inclination: (a) for the full range of particle shapes, (b) for the full range of particle-particle frictions, and (c) for the full range of particle-boundary frictions.

The symbols drawn on Figure 5(a) show the minimum and maximum velocity, where the shape of the particles was varied. Most of these symbols lie very close the curves for the DEM Base Case. The only notably exception is the simulation for the blockiest particles (case SQD) which produced the maximum swirl component and is an outlier when compared to all the cases. As the blockiest particle is likely to be a more extreme shape than that of the Japanese millet seed used in the experiment, it is then safe to conclude that all particle speed components are invariant to realistic variations in particle shape.

The symbols drawn on Figure 5(b) show the minimum and maximum velocity components where the particle–particle friction was varied. All of these symbols are extremely close to the curves for the DEM Base Case. So it is easy to see that all particle speed components are invariant to changes in particle–particle friction.

The symbols drawn on Figure 5(c) show the minimum and maximum velocity components where the particle–boundary friction was varied. All of these symbols again lie very close to the curves for the DEM Base Case. The only notable exception is that the swirl speed in a horizontal screw conveyor which increases modestly with increasing particle–boundary friction. For the remaining cases the particle speed components are all invariant to changes in particle–boundary friction.

POWER CONSUMPTION

Power consumption is determined from DEM predictions of the forces exerted by the millet seed particles on the rotating screw. For each operating condition, the screw conveyor reaches steady state operating conditions within 2–3 turns of the screw and the power draw is then quite steady.

Figure 6(a) shows the steady state power draw for the screw conveyor operating at 30% fill level and rotating at 1000 rpm, for various inclination angles. The four curves correspond to the 4 cases where the shape of the super-quadric particles was varied. The curves for the spherical particles are not shown here because they were co-linear with the curve for the Base Case. Figure 6(a) clearly shows that with increasing inclination angle the screw conveyor draws more power. Each of the four curves has the same shape. Initially, the increase in power is linear up to about 50°. The rate of change then declines leading to the power draw being independent of angle for inclinations above 80°. The rate of increase in power draw reflects the significant energy input required to increase and maintain the high swirl speeds observed at the higher screw angles. So as the inclination increases the transport rates achieved decline gently but the cost of maintaining the swirling motion in the uniform thickness bed flowing on top of the screw blade rises strongly.

Transport of particles that are increasingly non-round by the screw conveyor increases the power consumption. For example, comparing the Base Case with case SQC (which has particles that are more elongated) increased the power draw by about 9%. Comparing the Base Case with the elongated and blockier particles of case SQD shows an increase of the power consumption by about 20%. So even though the shape of the particles has little influence on the mass flow rates or the velocity components, the shape can

have a big influence on the power consumption of the screw conveyor. This will also correlate also with damage to the particles in transiting the screw conveyor.

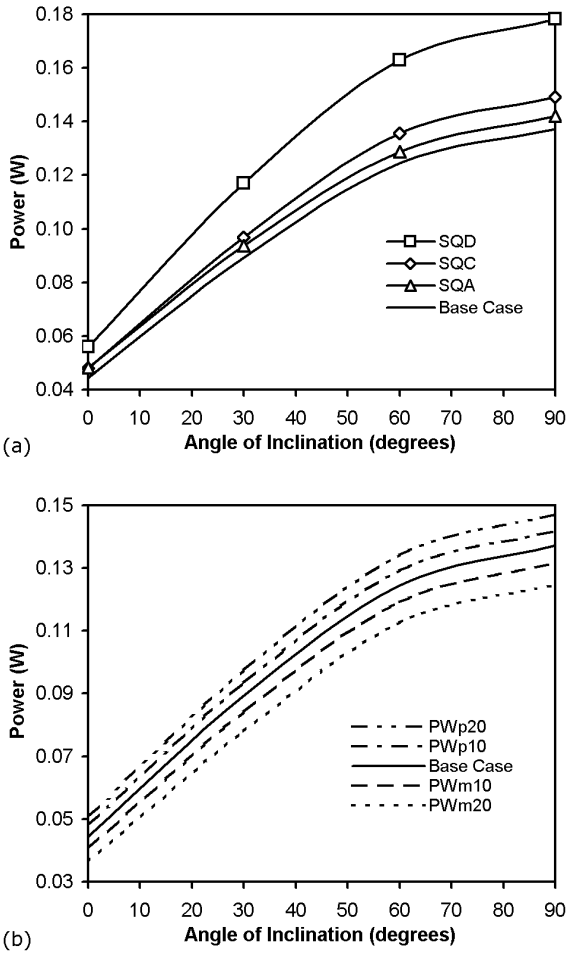

Figure 6: Power draw versus conveyor inclination: (a) for super-quadrics particles, and (b) for the full range of particle-boundary friction.

The five curves in Figure 6(b) shows the steady state power draw for the five cases where the particle–boundary friction was varied. The graph clearly shows that the power draw increases with steadily and consistently with increasing particle–boundary friction across the full range of inclinations. The average power scaling between these curves, when compared to the Base Case, are listed in Table 3. This indicates that there is an almost linear relationship between particle–boundary friction and the resulting power draw.

DEM Friction Cases	Particle-Boundary Friction	Average Power Scaling
PWm20:	0.40	-12%
PWm10:	0.45	-6%
SQB: (Base Case)	0.50	0%
PWp10:	0.55	5%
PWp20:	0.60	10%

Table 3: Power scaling with particle–boundary friction.

There was no noticeable difference between the power draw curves for the cases where the particle–particle friction was varied. They were all coincident with the curve for the Base Case. This indicates that inter-particle friction has negligible effect on the power draw.

CONCLUSION

The Discrete Element Method (DEM) has been used to explore the effect of particle shape and particle-particle and particle-boundary friction on transport performance in a screw conveyor.

We found that increases in non-sphericity have negligible effect on the particle flow patterns. The particle velocities and their axial and tangential (swirl) components were invariant to changes of particle shape and particle–particle and particle–wall friction. However, there were two notable exceptions. The first exception is the swirl velocity for the blockiest particles (case SQD), which was an outlier when compared to all other cases. As the blockiest particle is likely to be a more extreme shape than that of the Japanese millet seed used in the experiment, we can concluded that all particle speed components are invariant to realistic variations in particle shape. The second exception is that the swirl speed in a horizontal screw conveyor, which increases modestly with increasing particle–boundary friction.

In contrast to the invariance of the flow rates and velocities, the power consumption showed a reasonable dependence on particle shape and a modest dependence on particle–wall friction. The DEM simulations showed significant increases in power draw for increasing non-sphericity of the particles. Compared to the Base Case runs, the SQC runs, which have particles that are more elongated, predicted an increased power draw of about 9%. The SQD, with the elongated and blockier particles, predicted an increased power of about 20% when compared to the Base Case runs. So even though the shape of the particles has little influence on the mass flow rates or the velocity components, the shape can have a big influence on the power consumption of the screw conveyor. This will also correlate with damage to the particles in transiting the screw conveyor. The power consumption scales approximately linearly with the particle–boundary friction. Increasing the particle–boundary friction increases the power draw. Conversely, changes to inter-particle friction had no noticeable effect on the power draw.

The particle shape and particle property sensitivity studies were carried out to explore whether these were responsible for the differences between experiment results and DEM predictions for intermediate screw conveyor angles. It is clear that the shape of the particles and their frictional properties have negligible effect on all performance measures apart from the power draw. McBride and Cleary (2009) previously found excellent agreement between DEM prediction and experimental transport rates for a similar system across a very wide range of speeds when the particle shape and properties were included in the DEM model. The persistence of the differences for this system suggests that they are more likely to have their origin in the method of measurement used in the experiments. Roberts and Willis (1962) show a photograph of the apparatus used in their experiment. It is

not clear how they maintained consistent conditions at the downstream feed pool end of the conveyor for all angles of elevation. For a horizontal screw conveyor the millet seed is fed into the downstream pool from the top. However, when the screw conveyor is rotated to the vertical orientation, the seed is now fed from the side. Roberts and Willis also measured the "fullness" (volumetric fill level) of the grains in the screw conveyor by estimating the mean height of the seeds on the screw blade. The "fullness" at low screw conveyor inclinations would have been difficult to estimate because, as our flow pattern show, the layer of particles above the screw surface only becomes evenly spread out for inclinations above 30°.

REFERENCES

BORTOLAMASI, M., FOTTNER, J., (2001), "Design and sizing of screw feeders", *Proc. Partec 2001, Int. Congress for Particle Technology, Nuremberg, Germany, 27-29 March 2001*, Paper 69.

CLEARY, P.W., (1998a), "Predicting charge motion, power draw, segregation, wear and particle breakage in ball mills using discrete element methods", *Minerals Engineering*, **11**, 1061–1080.

CLEARY, P.W., (1998b), "Discrete Element Modelling of Industrial Granular Flow Applications", *TASK. Quarterly - Scientific Bulletin*, **2**, 385–416.

CLEARY, P.W., (2004), "Large scale industrial DEM modelling", *Eng. Comp*., **21**, 169-204.

CLEARY, P.W., (2007), "DEM modelling of particulate flow in a screw feeder", *Progress in Computational Fluid Dynamics*, **7**, 128–138.

McBRIDE, W, Cleary, P.W., (2009), "An investigation and optimization of the 'OLDS' elevator using Discrete Element Modelling", *Powder Technology*, **193**, 216-234

OWEN, P.J., CLEARY, P.W., MCBRIDE, B., (2003), "Simulated granular flow in screw feeders using 3D Discrete Element Method (DEM)", *CHEMECA 2003, 31st Australasian Chemical Engineering Conference*, ISBN 0-86396-829-5, Paper No. 203.

OWEN, P.J., CLEARY, P.W., (2009), "Prediction of screw conveyor performance using the Discrete Element Method (DEM)", *Powder Technology*, **193**, 274–288.

SHIMIZU, Y., CUNDALL, P.A., (2001), "Three-dimensional DEM simulation of bulk handling screw conveyors", *J. Engineering Mechanics*, September 2001, 864–872.

ROBERTS, A.W., Willis, A.H., (1962), "Performance of grain augers", *Proceedings of the Institution of Mechanical Engineers*, **176**, (No 8), 165–194.

ROBERTS, A.W., (1999), "The influence of granular vortex motion on the volumetric performance of enclosed screw conveyors", *Powder Technology*, **104**, 56–67.

YU, Y. AND ARNOLD, P. C., (1997), "Theoretical modelling of torque requirements for single screw feeders", Powder Technology 93, pp. 151–162.